Bachelor Thesis

Degree Project in
Geology 15 hp

The geochemical analysis of Yukon - Koyukuk basin clasts and their tectonic origin

Cecilia Nilsson

Stockholm 2017

Department of Geological Sciences
Stockholm University
SE-106 91 Stockholm
Sweden

Abstract

In 1989 Patton and Box first suggested that the Yukon Koyukuk basin is the relict of an intra-oceanic island arc that collided with continental North America in the late Jurassic to Early Cretaceous. The Koyukuk basin is a large wedge-shaped depression characterized by sequences of mafic to intermediate volcanic, volcaniclastic, and minor intrusive rocks. To test this hypothesis, major and trace element geochemical analysis of different clasts collected from the basin and the results were compared to those of the Koyukuk Terrain that already exist. The results indicate that the basin is in fact an intra- oceanic relict.

Table of contents

Introduction

The Yukon-Koyukuk Basin is a large (~250,000 km^2) wedge-shaped mid- and Late Cretaceous depression filled with sedimentary rocks (Fig.1). It is divided into two sub-basins, the Kobuk-Koyukuk and the Lower Yukon, which are separated by a structural high that exposes volcanic-arc rocks of the Koyukuk terrane (Patton and Box, 1989). Patton and Box suggested that the Koyukuk terrane was created in an oceanic setting by crustal thickening during intraplate magmatism. The oceanic plate then got subducted beneath this thickened crust and dipped away from the passive continental margin of North America, which resulted in the movement of the Koyukuk terrane toward the North American continent (Patton and Box, 1989). This is believed to have occurred from pre-Middle Jurassic to early Cretaceous (Box and Patton, 1989). This project uses geochemical data of conglomerate clasts collected from the basin, to test the hypothesis that the basin contains arc-derived detritus.

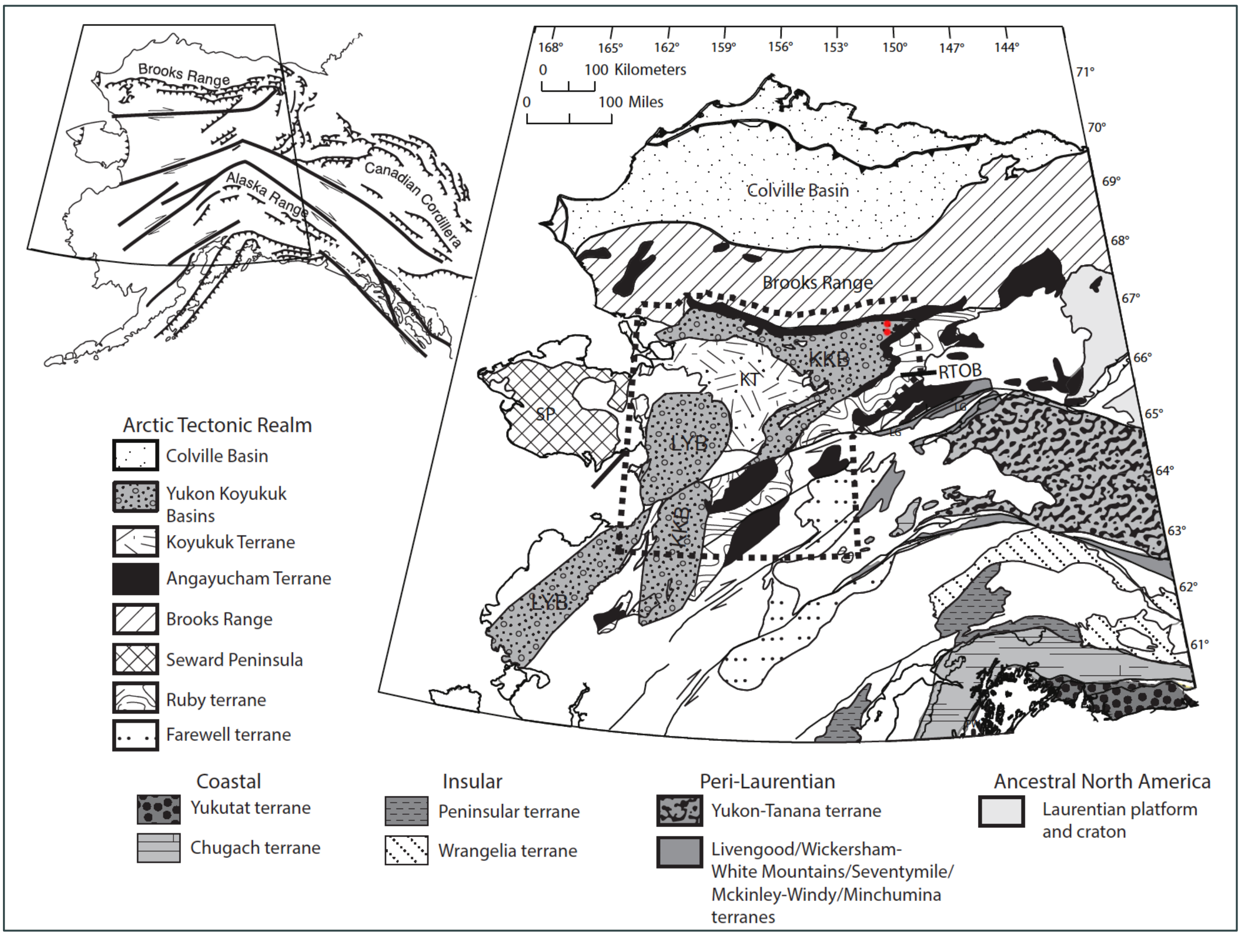

Figure 1. geological map of the Yukon – Koyukuk area (O'Brien et al., submitted). Red dots roughly represent the sampling location

Geological setting

An intra-oceanic arc occurs when a subduction zone develops within oceanic crust; they represent around 40% of the subduction margins on Earth today (Survey et al., 2003). When arcs like these close through collision with continental margins, it creates a distinctive structural and compositional record in continental orogens. The structure of the sedimentary rocks in the Yukon - Koyukuk Basin is complex due to the strong Cretaceous compression (Patton et al., 2009).

The Koyukuk terrane is overall characterized by sequences of mafic to intermediate volcanic, volcaniclastic, and minor intrusive rocks, and has been divided into four time-stratigraphic units (Fig.2) (Box and Patton, 1989). The whole basin is surrounded by highlands, to the north metamorphosed continental margin rocks and allochthonous oceanic accumulations of the Brooks Range, metamorphosed rocks of the Seward Peninsula to the west, and metamorphic rocks intruded by Cretaceous plutons to the southeast (O'Brien et al., submitted). The metamorphic mineral assemblages are mostly of greenschist facies, but an earlier, partly retrograded blueschist facies mineral assemblage can also be found (Box and Patton, 1989). North of the metamorphic belt in Brooks Range, a foreland fold and thrust belt occurs and it indicates northward transport, away from the Yukon-Koyukuk provinces (Box and Patton, 1989).

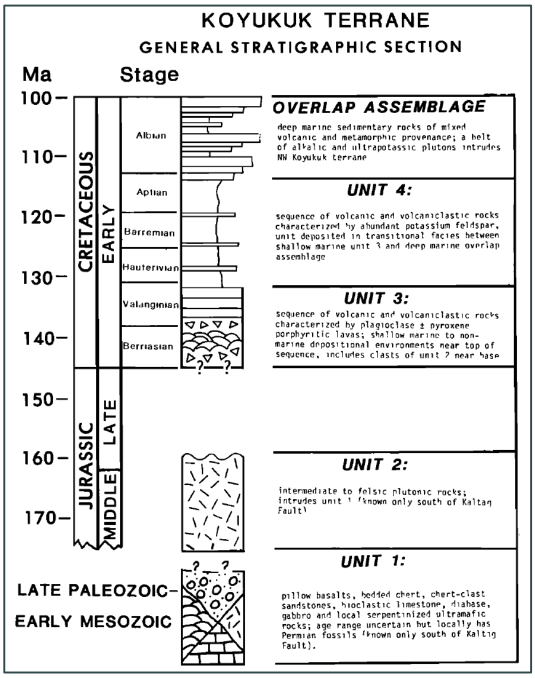

Figure 2. Generalized time-stratigraphic column for the Koyukuk terrane, showing approximate age range for units (Box and Patton, 1989)

Petrography

The samples are volcaniclastic clasts that are overall low grade metamorphosed (with a few exceptions) and has been overprinted by hydrothermal alteration characterized by the presence of calcite veins, chlorite and high amounts of oxides. The degree of alterations varies and the plagioclase was heavily altered in most of the samples and in some so much that they were unrecognizable. Hornblende was present in the samples VP16- 26f, VP16-26e and VP16-26b and could indicate amphibole facies. The presence of calcite is reflected in the high 'Loss on Ignition'(LOI). More of the LOI is discussed below in Table 1. The clasts are melanocratic and a bit greenish in color, mostly an aphanitic texture, but some are more phaneritic. For more information about each sample See appendix.

Analytical methods

The analytical methods that was used was X-ray fluorescence (XRF) and Inductively coupled plasma mass spectrometry (LA – ICP- MS) for chemical analysis of major and trace elements.

Sample preparation

The samples were prepared by first removing the weathered edges with a saw and then removing any steel from the saw by coarse polishing. After cleaning, the samples were crushed into smaller pieces (under 9mm) and then turned into a powder by the disk mill. A Vibratory Disk Mill (RETCHET RS200) was used to generate the final sample powder to be used for x-ray fluorescence (XRF) and laser ablation inductively coupled plasma mass spectrometry (LA-ICP-MS) analysis.

XRF

The XRF provides particularly accurate major element (oxide) analyses, with good reproducibility and precision for most elements. Such chemical analyses are used for a variety of studies, from experimental mineralogy and micro-structural analysis to igneous and metamorphic petrology. Structurally bound water is driven off the samples first by the LOI process, where 5g of the sample is put inside a crucible placed inside an oven at c. 1000 degrees for three hours. The LOI results are provided in the appendix. After this step, the samples are fused into glass disks for XRF analysis; the samples are mixed with lithium metaborate flux at 5 parts flux: 2 parts dehydrated sample powder, which assists fusion by lowering the melting temperature. The machine used to melt the samples is the automated Phoenix auto-fuser, ensuring that every sample is treated in the same manner.

LA – ICP – MS

After the XRF analysis is complete and its quality assessed, the glass disks are crushed and a small piece is selected for LA-ICP analysis. The LA-ICP-MS at Stockholm University can be used for the analysis of fluid inclusions, U-Pb dating, and trace element concentrations of silicates. The instrument operating conditions used are given below.

Table 1. LA-ICP-MS operating conditions

Analytical conditions
Laser energ 7.3 J/cm2
Spot size: 150 µm
frequency: 10 Hz
Additional 11.1 ml/min

5 analyses per sample
External sta NIST-612
Secondary s BCR-2 / SARM-1
Internal star Si
20 seconds background, 40 seconds laser-on, 10 seconds wash-out

Analytical results

Geochemistry

The samples are a mixture of meta-sediments and volcanic rocks (Table 2), but only the volcanic rocks are further studied in this thesis. The geochemical analyses are presented in Table 3. The volcanic samples are classified below into rock types, magma series, and tectonic setting determined from their chemical composition. Spider diagrams normalized to EMORB and Rare earth element diagrams was also made to identify characteristics and signatures in the geochemical data. Normalization data taken from Sun and McDonough, 1989 (Fig.5-6)

Table 2. Koyukuk Basin clast types.

Volcaniclastic sediment	**Basalt**	**Andesite**	**Trachy-andesite**
VP16-25e	VP16-25g	VP16-25f	VP16-26f
VP16-26c	VP16-26b	VP16-26a	
VP16-26d	VP16-26e		

Classification

Rock type was determined using the chemical classification diagram for volcanic rocks which is based on total alkalies [Na2O + K2O] vs. SiO2. The samples include basalts and andesites, except for one outlier (VP16-26a) which is a Trachy-andesite (Fig. 3).

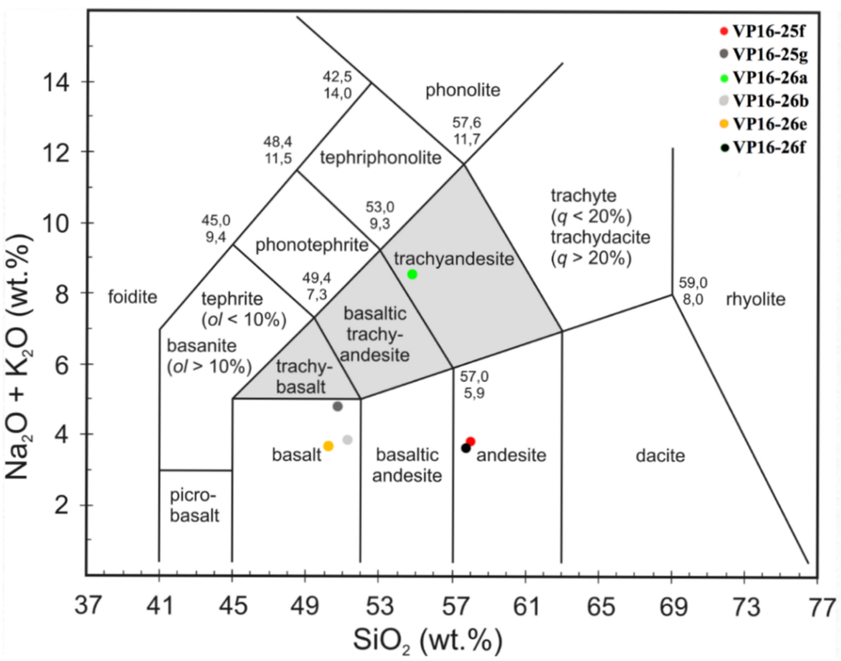

Figure 3. Sample classification in weight percent oxide. Note the samples represent basalt, andesite, and a single trachy-andesite.

Table 3. Geochemical analyses of Koyukuk Basin clasts.

Major and trace element analyses

Sample ID	VP16-25e	VP16-25f	VP16-25g	VP16-26a	VP16-26b	VP16-26c	VP16-26d	VP16-26e	VP16-26f
Major elements (wt%)									
SiO2	78.6	58.3	50.9	54.6	50.8	83.7	69.5	49.8	58
Al2O3	9.24	15.8	17.1	18.7	16.2	8.04	11.6	17.1	15
CaO	0.429	5.35	8.31	4.88	9.65	0.34	2.83	10.4	10.1
MgO	1.95	4.42	3.36	4.65	5.99	0.92	2.98	7.28	6.72
MnO	0.065	0.252	0.238	0.205	0.216	0.019	0.086	0.175	0.147
P2O5	0.072	0.25	0.16	0.084	0.098	0.046	0.079	0.037	0.013
Fe2O3	6.74	10.5	13.2	7.37	11.8	4.45	9.33	10.5	6.03
Na2O	0.597	3.11	4.29	5.65	3.16	0.768	2.09	2.71	3.03
K2O	1.38	0.709	0.465	3.03	0.705	1.05	0.743	1.03	0.623
TiO2	0.896	1.23	1.99	0.768	1.38	0.683	0.769	0.933	0.399
Total	100	100	100	100	100	100	100	100	100
LOI	3%	4.4%	6.9%	4.7%	1.8%	2.1%	4.8%	1.9%	1.6%
Trace elements (ppm)									
Ba	294.1	185.8	272.3	455,00	645.6	202.5	146.6	1728.6	141,00
Cr	363.7	111.7	44.1	113,00	104.3	232.2	345.5	127.3	314.7
Cs	2.44	0.0748	0.605	0.0623	0.874	1.95	1.58	0.97	0.125
Cu	26.3	206.6	117.1	6.12	154.6	103.6	181.8	155.7	11.53
Ga	10.8	14.9	18.7	11.6	15.7	10.03	10.43	13.1	11.33
Hf	12.5	3.09	3.36	2.63	2.08	9.16	5.84	1.18	1.11
Nb	14.6	2.653	3.75	1.73	2.04	11.8	9.35	0.998	0.979
Ni	60.3	24.7	16.4	37.3	38.05	<44.38	130.1	50.9	79.3
Pb	2.92	3.08	3.15	3.77	1.27	7.34	8.2	0.764	1.15
Rb	53.9	7.4	7.96	28.7	12.9	46.6	26.2	19.21	10.8
Sc	16.34	33.2	41.3	31.8	42.9	14.4	17.5	43.65	35.5
Sr	22.1	259.9	327.6	146.7	404.7	43.2	71.1	294.3	312.5
Ta	1.233	0.168	0.22	0.13	0.12	0.912	0.611	0.07	0.0613
Th	16	1.15	0.919	0.716	0.368	11.7	5.43	0.273	0.539
U	3.42	0.632	0.354	0.326	0.182	2.58	1.5	0.119	0.296
V	111.1	285.4	464	178.6	331.9	79.2	124.6	275.1	133.5
Y	28.71	34.9	28.4	22.71	25.4	26.7	19.53	15.8	10.27
Zr	450.3	99.6	119.1	90.1	73.7	332.4	227.9	39.8	42.5
La	4.05	13.87	9.28	7.67	6.19	29.26	4.82	2.79	3.84
Ce	9.87	33.17	20.3	17.79	14.15	60.03	12.84	6.69	7.51
Pr	1.39	5	3.14	13.3	2.247	6.88	1.886	1.11	0.952
Nd	6.8	24.5	15.5	3.54	11.7	27.3	8.82	5.9	4.24
Sm	2.16	6.55	4.61	0.933	3.7	5.48	2.58	2.04	1.29
Eu	0.575	1.77	1.69	3.82	1.36	1.02	0.688	0.826	0.515
Gd	3.38	6.64	4.9	0.644	4.1	4.75	2.98	2.51	1.46
Tb	0.692	1.07	0.914	4.15	0.719	0.807	0.56	0.435	0.268
Dy	4.95	6.51	5.84	0.878	4.9	4.87	3.53	3.02	1.86
Ho	1.11	1.38	1.22	2.66	1.006	1.04	0.759	0.646	0.396
Er	3.36	3.80	3.65	0.399	2.92	2.99	2.171	1.79	1.155
Tm	0.519	0.5234	0.51	2.79	0.389	0.414	0.315	0.263	0.163
Yb	3.54	3.78	3.72	0.409	2.86	3.01	2.25	1.77	1.3
Lu	0.547	0.546	0.515	0.409	0.407	0.43	0.334	0.261	0.191

Notes: Trace elements were analyzed by LA-ICP-MS. Analytical accuracy and precision were evaluated using international reference standards. Relative standard deviations are <0.2% for SiO2 and <1% for the other major elements, except MgO, TiO_2 2% and P_2O_5 4.2%. Relative standard deviations for trace elements are mostly ~5% (Ta has a higher STD at 14%). Structurally bound H2O was determined by measurement of loss on ignition (LOI). Abundances indicated by '<'=below determination limits. Ni for sample VP16-26d had a limit of detection at 120 ppm.

The magma series is used to determine the melt source and if the samples might represent a cogenetic suite. This is defined with an AFM diagram (Fig. 4a). Most of the samples are tholeiitic, excluding VP16-26a and VP16-26f which are calc-alkaline (Fig. 4a). Furthermore, the tectonic setting can be determined using the discrimination diagram of ratios of some minor and trace elements to indicate the original source of mafic volcanic rocks (Winter, 2013) and all the Koyukuk Basin volcanic clasts are island arc basalts (Fig. 4b).

Figure 4. A) Magma series classification. Note most samples are tholeiitic. Two samples are calc-alkaline. B) Tectonic classification. Note that all samples represent island arc basalts (IAB).

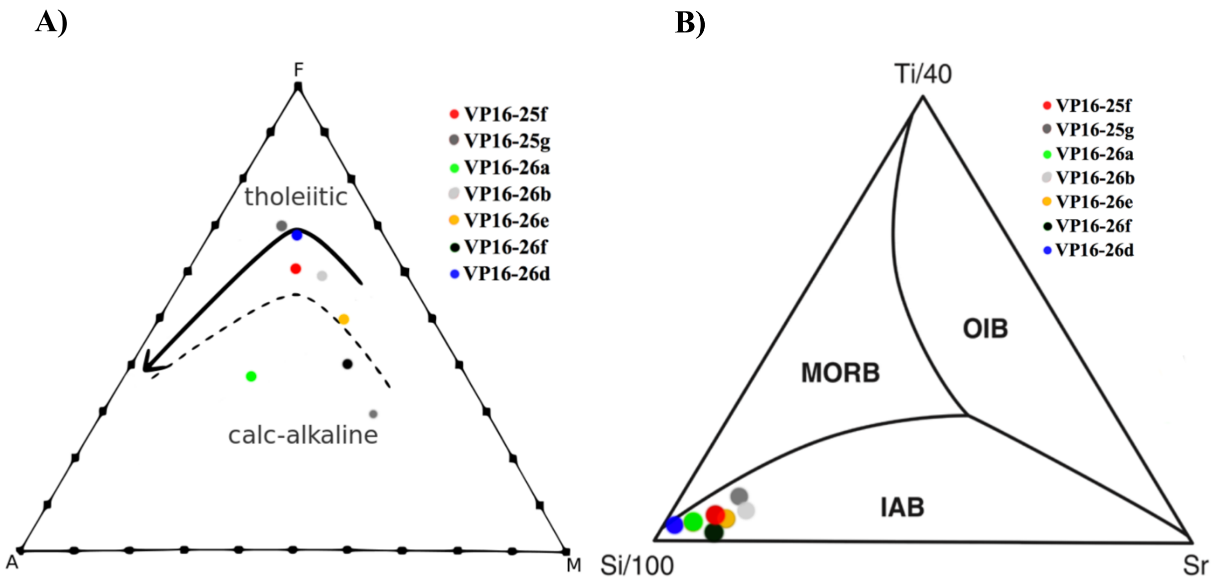

Discussion

Most of the geochemical data and classifications indicate that the samples are in fact from an intra-oceanic subduction zone. These results are summarized in Table 4.

Table 4. Summary of magma series and tectonic environment.

Tholeiitic	Calc-alkaline	IAB
VP16-25g	VP16-26a	VP16-25g
VP16-26b	VP16-26f	VP16-26b
VP16-26e		VP16-26e
VP16-25f		VP16-25f
VP16-26d (sed)		VP16-26a
		VP16-26f
		VP16-26d (sed)

Three of the samples were identified as volcaniclastic sediment in thin section and therefore they require a different classification scheme relative to the volcanic samples. These have been plotted in a discriminant function diagram for the provenance signatures of sandstones- mudstone suites using major elements (Appendix). A single meta-sediment sample has a mafic provenance and its chemistry matches with the volcanic rocks; it was therefore decided to plot it with the volcanic samples due to its common geochemical characteristics - it is shown as a dotted line on all subsequent graphs.

The geochemistry of the volcanic samples suggests that they formed in an island arc (IA) tectonic environment. This supports the intra-oceanic subduction hypothesis of Patton & Box (1989). The classification diagrams show an assemblage typical of IA settings, with a tholeiitic to calc-alkaline magma series and IA signatures (Fig. 4). These features indicate a less-evolved magma series which could reflect the early stage of subduction. The magma becomes more and more evolved as the subduction system develops and the subducting slab reaches greater depths (tholeiitic to alkaline).

To further investigate the samples they have been normalized to chondrite, MORB and Primitive mantle (Sun and McDonough, 1989) to assess potential correlations (see the appendix for all figures). The best-fit is derived from the normalization with EMORB, which shows an almost flat trend, around unity (Fig. 5).

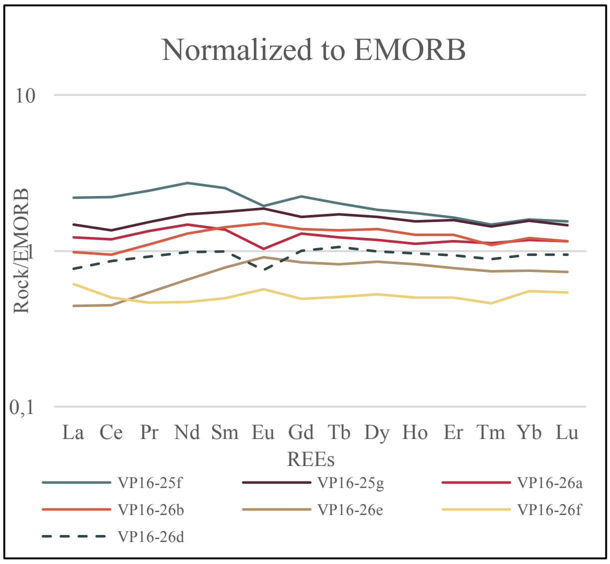

Figure 5. Rare earth element diagram normalized to EMORB. Using the normalization and ordering scheme of (Sun and McDonough, 1989)*), with increasing compatibility to the right.*

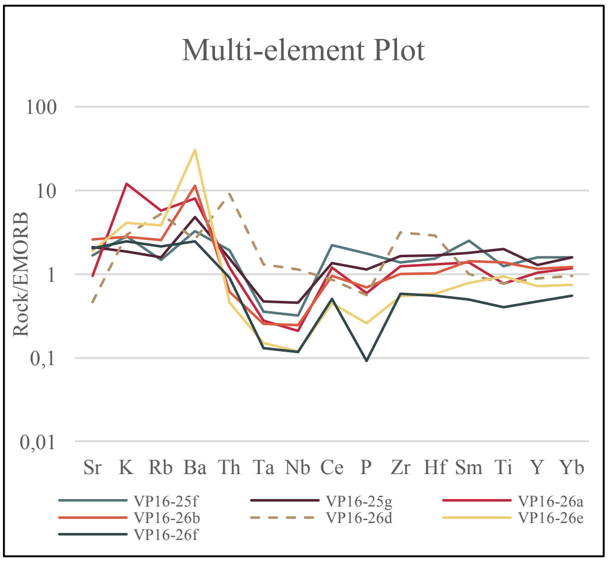

Figure 6. Multi-element spider diagram normalized to EMORB. Using the normalization and ordering scheme of (Sun and McDonough, 1989)*), with LIL on the left and HFS on the right and compatibility increasing outward from Ba-Th.*

The normalized multi-element plot shows only a weak 'subduction' geochemical fingerprint (Fig. 6). A subduction fingerprint is identified as a negative anomaly in Nb (a depletion in Nb/Ta relative to LREE) and an enrichment in the fluid-mobile elements such as LREEs (La/Lu values above 1). The Nb anomaly is not as pronounced as it is in the modern Andean margin and together with their tholeiitic composition seems to confirm that these IA samples likely represent the early phase of subduction initiation.

The rocks in unit 2, 3a, 3b, and 3c, (Fig. 2) are the rocks that most resembles lavas of an island arc. Basalts and basaltic andesites dominates, they are mostly of tholeiitic character, and have a gently light-enriched REE pattern (Box and Patton, 1989). This is reflected in the classification results.

In thin section, some of the samples clearly document amphibolite facies. According to Patton and Box (1989) the earliest subduction-related magmatism is recorded by the calc-alkaline plutons of unit 2, that had been eroded away during the Late Jurassic uplift. Convergent tectonism connected with this arc magmatism is defined by amphibolitic tectonites. These tectonites occur in the middle of mafic oceanic rocks which suggests that this tectonism occurred within an oceanic plate realm and is related to oceanic subduction beneath the Koyukuk terrane. The bivariate plots lack the linear trends that indicate crystal fractionation played the dominant role generating this magma series – this means that the relationships between samples are not due to undifferentiated partial melt, but magma mixing may be the dominant mechanism instead. Magma mixing is a common process in most volcanic systems and is the main mechanisms for generating andesites and trachy-andesites (Reubi and Blundy, 2009) It is possible that these samples represent a mix between two different magmas. None of the Koyukuk samples from Box and Patton (1989) had the characteristics of a crystal fractionation of mantle material, and none could represent the parental melt composition. So, the results aren't surprising. With further research and isotopic data, the source compositions could maybe be identified.

Conclusions

- The metasedimentary sample that had a similar chemical signature as the mafic samples was probably originally the same type of rock but has been altered by weathering and erosion which altered its chemical composition and texture.
- The tholeiitic to calc-alkaline characteristics, IA signature and subduction fingerprint are the results that best shows that the clast has an intra-oceanic subduction origin.
- No linear trend in the bivariate plots shows that crystal fractionation is not the main mechanism and that it has been overprinted by magma mixing instead. And to determine the composition of the parental melt more research and isotropic data is needed.
- With the low number of clast available, there is not enough data to come to a full conclusion. But it is enough data to emphasize the theory that Patton and Box suggested that the Yukon – Koyukuk basin is in fact a relic from an intra-oceanic subduction zone.

Acknowledgments

First I want to thank my supervisor Victoria Peace who for all the help and support, for always having time to answer questions and steering me in the right directions. I also want to thank Emelie, Dan and Kurt for helping me with all the lab works and sample preparations. Lastly but not least I want to thank Agata and Charlotte for the support and for making this process a lot more fun.

References

Box, S.E., and Patton, W.W., 1989, Igneous history of the Koyukuk Terrane, western Alaska: Constraints on the origin, evolution, and ultimate collision of an accreted island arc terrane: Journal of Geophysical Research, v. 94, p. 15843, doi: 10.1029/JB094iB11p15843.

Patton, W.W., and Box, S.E., 1989, Tectonic setting of the Yukon-Koyukuk Basin and its borderlands, western Alaska: Journal of Geophysical Research, v. 94, p. 15807–15820.

Patton, B.W.W., Wilson, F.H., Labay, K.A., and Shew, N., 2009, Geologic Map of the Yukon-Koyukuk Basin , Alaska: : U.S. Geological Survey Scientific Investigations Map 2909, scale 1:500,000, 2 sheets and pamphlet [https://pubs.usgs.gov/sim/2909/].: USGS Pamphlet,.

Reubi, O., and Blundy, J., 2009, A dearth of intermediate melts at subduction zone volcanoes and the petrogenesis of arc andesites: Nature, v. 461, p. 1269–1273, doi: 10.1038/nature08510.

Sun, S. -s., and McDonough, W.F., 1989, Chemical and isotopic systematics of oceanic basalts: implications for mantle composition and processes: Geological Society, London, Special Publications, v. 42, p. 313–345, doi: 10.1144/GSL.SP.1989.042.01.19.

Survey, B.A., Cross, H., and Road, M., 2003, Intra-oceanic subduction systems : introduction: , p. 1–17.

Winter, J.D., 2013, Principles of Igneous and Metamorphic Petrology: Pearson New International Edition: 738 p., https://books.google.be/books?id=HBWpBwAAQBAJ.

Appendix

Thin Section Descriptions

VP16 – 25e
Whole Rock: Sedimentary origin, Layering – gradual size layers– 70% Quartz, 10% Chlorite, 20% Groundmass
Major elements: Quartz, Chlorite
Minor elements: K-feldspar (Plagioclase), Muscovite, Epidote, Oxides
Textures/Reactions: Sericite
Description: Big quartz crystals (kind of rounded) surrounded by a groundmass of chlorite and other altered minerals, Few but quite big grains of epidote, muscovite and feldspar

VP16-25f
Whole Rock: Phaneritic, Mesocratic, 50% Plagioclase, 40% Chlorite, 10% Quartz
Major elements: Chlorite, Quartz, Plagioclase
Minor elements: Oxides, Sericite
Textures/Reactions: Sericite, Myrmekite
Description: Big altered (sericite) plagioclase grains, surrounded by chlorite and small grains of quartz

VP16-25g
Whole Rock: Melanocratic, Aphanitic to phaneritic (finer grained), 50% Feldspar, 40% Chlorite
Major elements: K-Feldspar (Sanidine), Quartz, Chlorite
Minor elements/ Accessory: Olivine, Calcite, Oxides
Texture/Reactions: Zoning, Calcite veins
Description: Chlorite crystals and chlorite replacing other minerals. Calcite veins and chlorite indicates hydrothermal alteration.

VP16-26a
Whole Rock: Phaneritic, mesocratic green, 50/50 grains and ground mass, Groundmass – 100% feldspar, Grains – 70% feldspar, 15% Chlorite, 15% Epidote
Major elements: K-Feldspar, Chlorite, Epidote
Minor elements/Accessory: Calcite, Sericite, Oxides
Textures/Reaction: Epidote inclusion in Feldspar
Description: Big grains of feldspar, calcite and chlorite surrounded by a groundmass – typical trachy- texture, Calcite, Calcite veins and chlorite indicates hydrothermal alterations.

VP16-26b
Whole Rock: Phaneritic, Mesocratic green, 50% Feldspar, 35% Amphibole, 15% OPX
Major elements: K-Feldspar – Plagioclase, Amphibole (Hornblende), OPX, Quartz
Minor elements/accessory: Myrmekite, Oxides
Textures/Reactions: Zoning, OPX starting to be replaced by chlorite
Description: Big happy Hornblende grains, big quite happy opx grains – very similar but color and cleavage is different. Amphibole indicates hydrothermal alterations.

VP16-26c
Whole Rock: Sedimentary origin, 85% quartz
Major elements: Quartz
Minor elements/accessory: Chlorite, Plagioclase, Epidote, Biotite, Muscovite
Textures/Reactions:
Description: Very fine grained, Quartz dominates, a few grains of mica, epidote, plagioclase

VP16-26d
Whole Rock: Sedimentary origin, 85% quartz
Major elements: Quartz
Minor elements/accessory: Plagioclase, Biotite, Epidote, Calcite, Muscovite
Textures/Reactions: Calcite vein
Description: Very fine grained, very alike the VP16-26c sample with less chlorite/serpentine, altered cracks, Faulting, Layering – bigger/smaller grains of quartz, Rounded quartz grains
VP16-26e
Whole Rock: Phaneritic, Mesocratic
Major elements: Plagioclase, Amphibole (Hornblende), Chlorite, Pyroxene
Minor elements/accessory: Sericite, Oxides
Textures/Reactions: Zoning, Pyroxene being replaced by chlorite?
Description: Big amphibole grains, some very unhappy (Could be the pyroxene) Big altered plagioclase grains – almost impossible to identify
VP16-26f
Whole Rock: Mesocratic – 50/50 Dark light minerals
Major elements: Quartz, Chlorite, OPX, Amphibole (Hornblende), Calcite, Plagioclase
Minor elements/accessory: Sericite
Textures/Reactions
Description: Big crystals black from alteration – probably altered plagioclase

Graphs

QAP diagram to further classify the samples

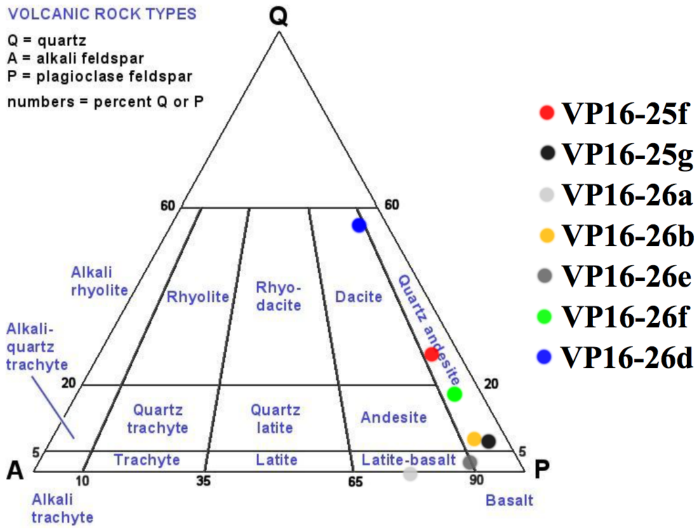

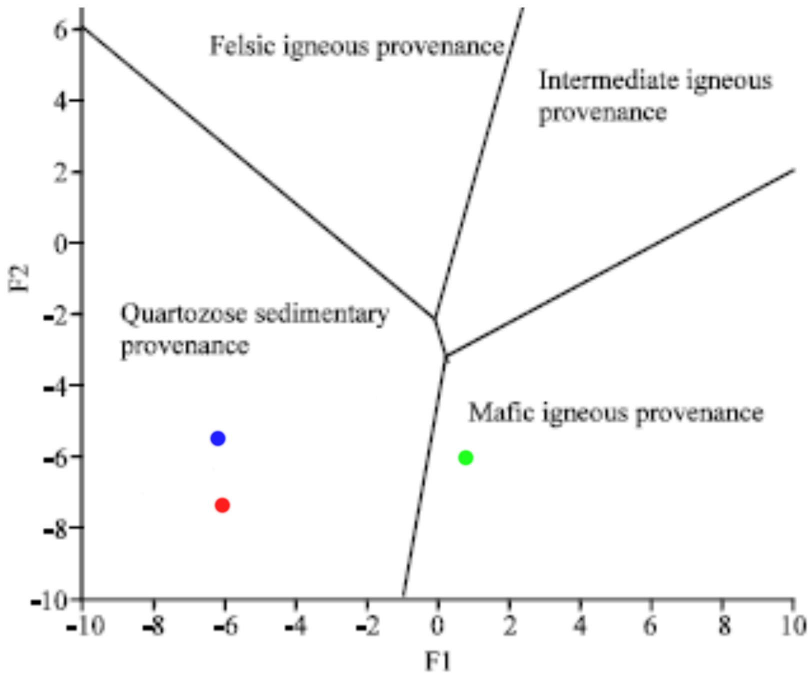

Discriminant function diagram for the provenance signatures of sandstones- mudstone suites using major elements.

Normalized Chondrite compared to data from Box and Patton (1989). The graph show some similarities with Unit 3b

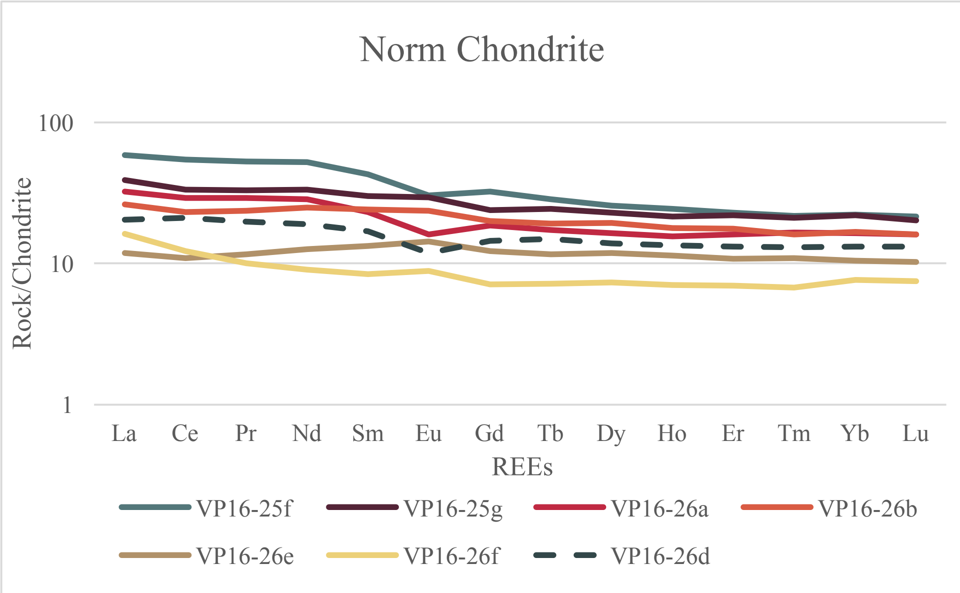

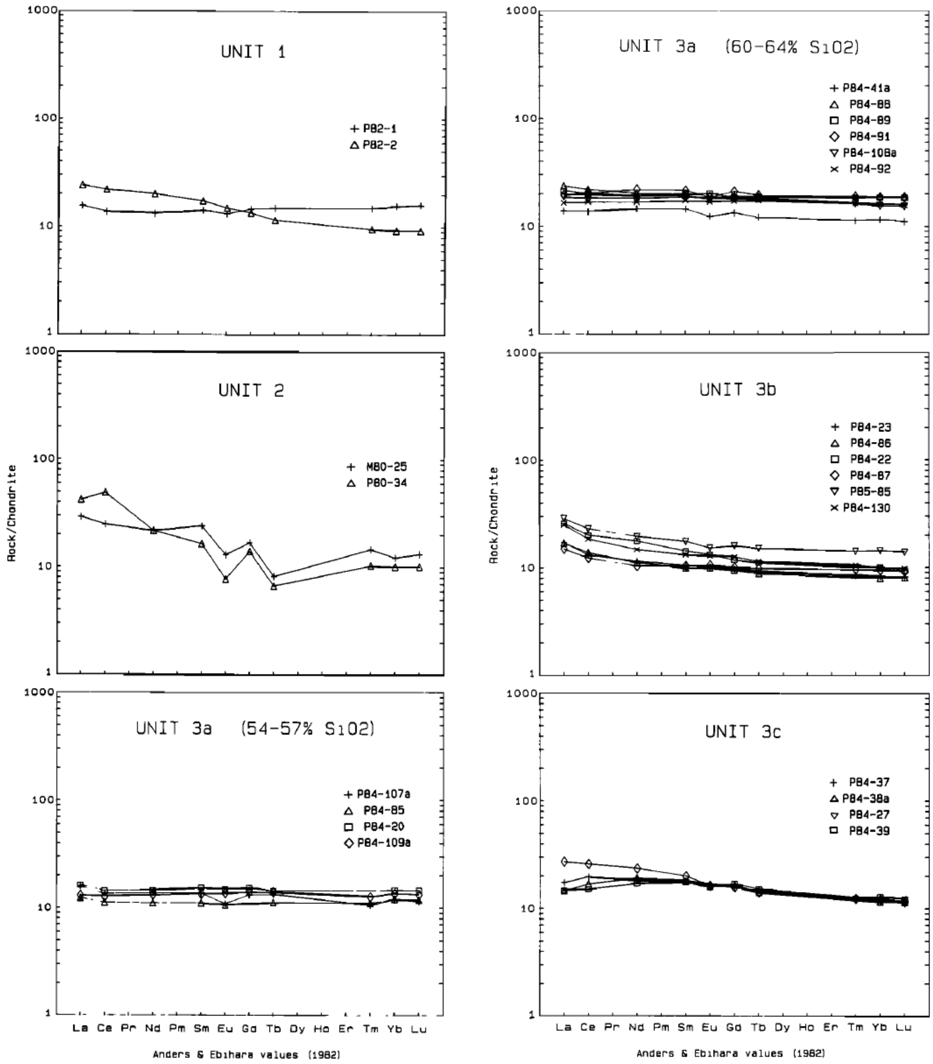

Multi element plots showing the samples normalized to Chondrite (Box and Patton, 1989). The graphs shows almost no similarity with the data from Box and Patton (1989)

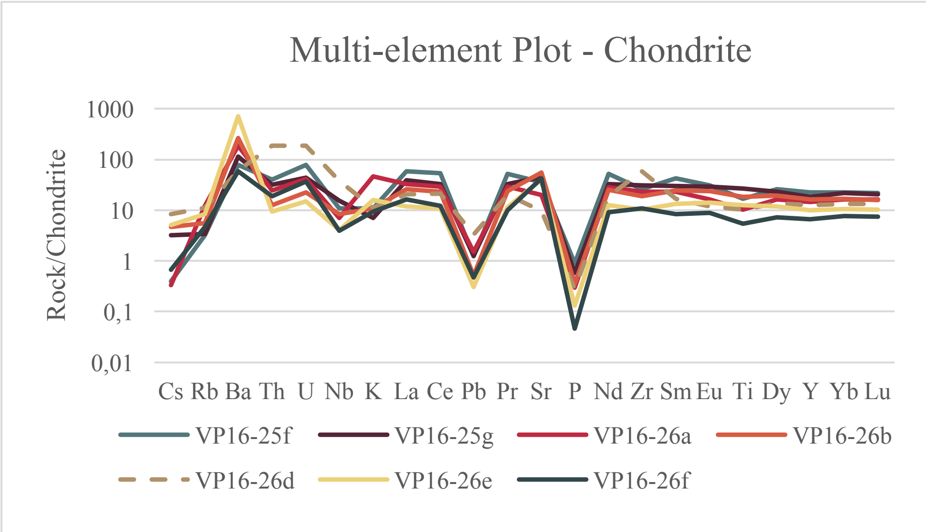

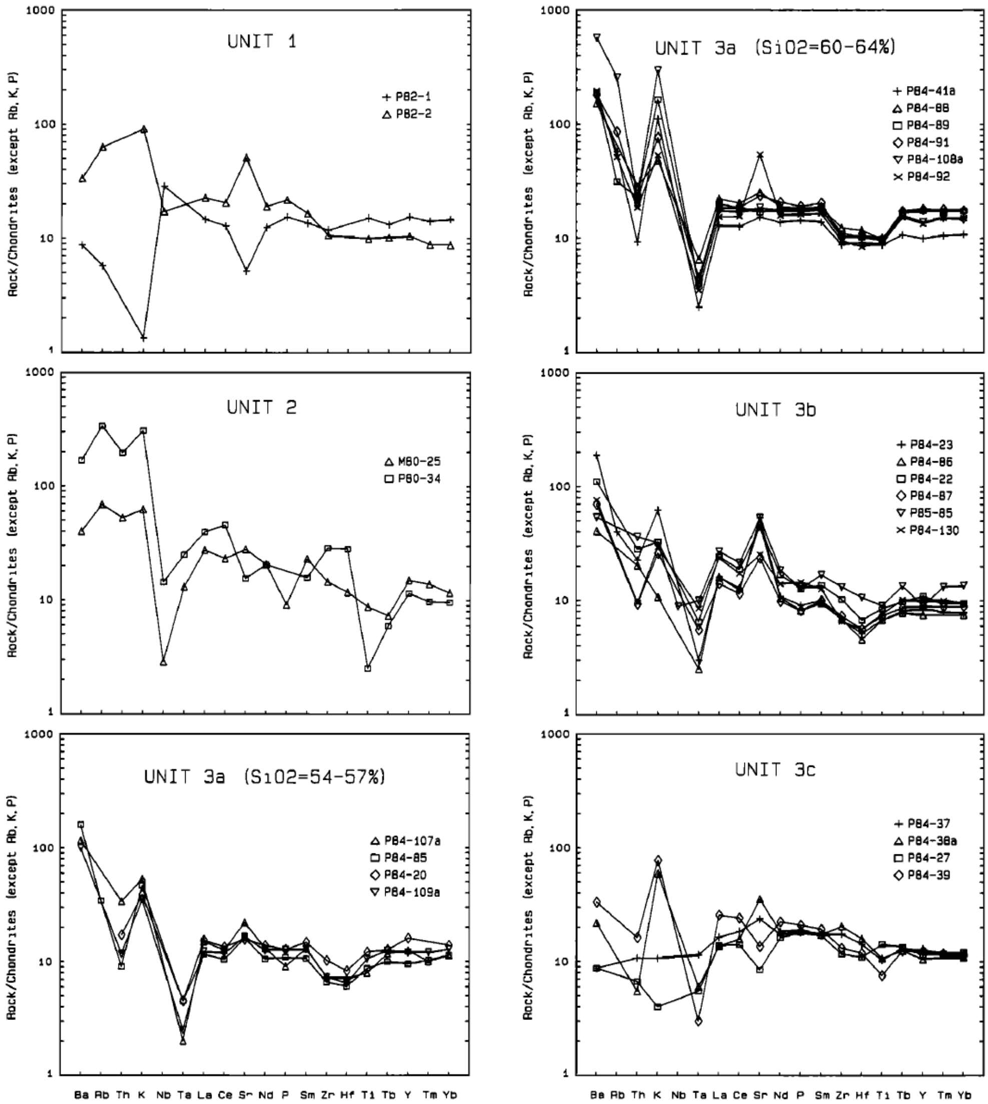

Harker variation diagrams. wt. % silica plotted against the major oxides. As seen the samples do not follow a linear trend that is associated with dominant crystal fractionation.